Optimum design of the drive-coil for a 500J inductive pulsed plasma thruster and its numerical evaluation

IEPC-2019-A-158

Presented at the 36th International Electric Propulsion Conference
University of Vienna • Vienna, Austria
September 15-20, 2019

Bixuan Che[1], Mousen Cheng, Xiaokang Li, Dawei Guo and Moge Wang
College of Aerospace Science and Engineering, National University of Defense Technology, Changsha, Hunan, 410073, China

Abstract: The National University of Defense Technology is now undertaking the development of an IPPT prototype with single pulse energy ranking about 500J (eight 1μF capacitors charge to 12kV). This paper introduced the preliminary design works of that device, whose content mainly include the optimization of the drive-coil geometry and the numerical evaluation of the design result. Since drive coil plays as the mediate coupling the plasma load and the pulse circuit, a proper design of the coil geometry, including both coil configuration and dimension, turns out to be the key to achieve high efficiency. Based on the classical lumped slug model and comprehensive considerations of drive-coil EM field properties, we optimized the inner and outer radii of drive-coil. The requirement of azimuthal electric field for an efficient breakdown at initial occasion is considered as a restrict bound on the inner and outer radii. To evaluate the design result, a two-dimensional magnetohydrodynamic model coupled with drive-circuit is employed to simulate the working process. This numerical model has demonstrated its validity and veracity to simulate an IPPT in our earlier research works. The result indicate that, the designed IPPT device can accelerate about 0.75mg of Argon propellant with a specific impulse of 2240s and an efficiency around 30%.

I. Introduction

The inductive pulsed plasma thruster (IPPT), which inductively and impulsively exhausts bulks of plasma at high velocity (about 10km/s) to generate thrust impulses, is a sort of electromagnetic plasma accelerator applied in in-space propulsion. Owes to its unique electrode-less nature, IPPT is free from lifetime or contamination issues related with electrode erosion and is capable of handling high power levels up to megawatt as well as adopting "cheap" propellants like NH_3 and CO_2. These features make it one of the most promising candidates for deep space missions such as manned Mars exploration and lunar cargo transport[1]. The concept of IPPT was first proposed by Dailey and Lovberg in the 1960s and is now investigated by research groups around the world[2-6].

As is shown in Figure 1, a typical IPPT consists of a gas injector, a switch, a capacitor and a flat annular spiral drive-coil. The conductors of drive-coil are embedded in insulating material to avoid direct contact with plasma. The capacitor and switch are mounted on the back of a metal shielding plate to protect them from the strong electromagnetic (EM) field induced by drive-coil. IPPT works in pulsed mode: before triggering the switch, a layer of neutral gas is delivered to the surface of drive-coil from the gas injector; then the switch is triggered and a strong and short current pulse is formed in drive-coil; after that, a time-varied EM field is induced, which contains azimuthal electric field E_θ and radial magnetic field B_r; E_θ breaks down the neutral gas and drives a current sheet which carries enclosed azimuthal plasma current density $J_{p,\theta}$; the current sheet is then repelled axially away by the Lorentz body force F_{ltz} that arises from the interaction between $J_{p,\theta}$ and B_r.

[1] PhD candidate, College of Aerospace Science and Engineering, National University of Defense Technology, chebixuan@outlook.com.

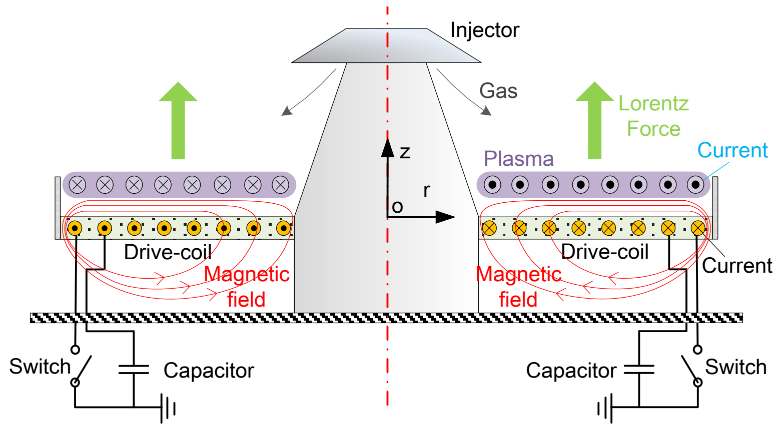

Figure 1. Schematic plot of IPPT

The National University of Defense Technology is now undertaking the development of an IPPT prototype with single pulse energy ranking over 500J (eight 1μF capacitors charging to over 12kV). This paper introduced the preliminary design works of that device, whose content mainly includes the optimization of the drive-coil dimension and the numerical evaluation of the design result with a circuit coupled MHD method.

II. Optimization method

A. Optimization flow

The performance of an IPPT highly relies on two physical processes within each single discharge pulse: the ionization of neutral gas at the beginning of discharge, and the acceleration of plasma current sheet during the period of discharge[1,5]. As for the ionization of neutral gas, considering a single stage IPPT without pre-ionization method, the initial plasma is produce by gas breakdown under E_θ at t=0. Any delay of gas breakdown or inefficiency of early ionization would lead to the failure of producing a magnetic impermeable plasma current sheet, and as a result, the ultimate acceleration of plasma might be impaired. As for the acceleration of plasma current sheet, the time periods of both circuit current waveform and plasma current sheet movement should meet a so-called "dynamic impedance match" condition, where the efficiency of the thruster achieves the maximum[7].

Taking aforementioned two processes into consideration, we optimized the inner radii r_1 and outer radii r_2 of drive-coil following the steps shown Figure 2. For a certain r_1/r_2, the EM properties of drive-coil including its inductance L_C, decoupling distance z_0 and E_θ (at t=0 along the central lines between r_1 and r_2) were calculated based on theoretic equations. The classical lumped slug model was adopted to estimate the performance parameters including specific impulse I_{sp} and efficiency η. Varied mass bit m_{bit} values were compared to find an optimum one whose η was maximum for that given r_1/r_2. These procedures were re-performed for varied r_1/r_2 combinations and consequently, the contour maps of E_θ, I_{sp} and η using r_1 and r_2 as the axes were figured out.

Meanwhile, E_θ of those effective IPPTs ever reported in references were calculated using the same method to provide threshold that our design should achieve. After that, depending on the contour map of E_θ, a restrict region of r_1 and r_2 to guarantee a sufficient initial ionization was drawn out. Within this restrict region of r_1 and r_2, the optimum r_1/r_2 values were determined.

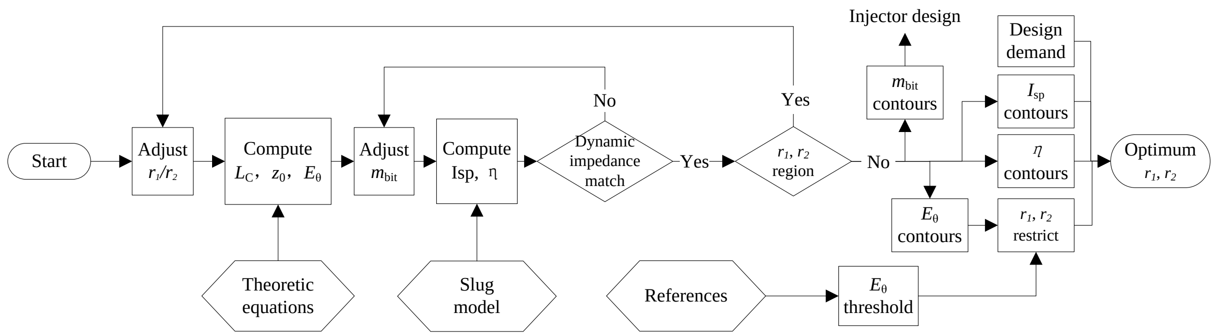

Figure 2. Optimization flow chart

B. Drive-coil EM property

The fundamental drive coil geometry is illustrated in Figure 3, which consists of 16 groups of 1-turn 2π Archimedes spiral line conductors connected in parallel and arranged axisymmetrically. The geometry of spiral lines can be describe by:

$$r = r_1 + k\theta, k = \frac{r_2 - r_1}{2\pi} \quad (\theta = 0 \sim 2\pi) \tag{1}$$

The electromagnetic property of drive-coil assembly can be rather well replaced by a consecutive current sheet, where the distribution of azimuthal current density j_C can be derived depending on the spiral line geometry:

$$j_C = \frac{I_1}{(r_2 - r_1)} \cdot \frac{r}{\sqrt{k^2 + r^2}} \tag{2}$$

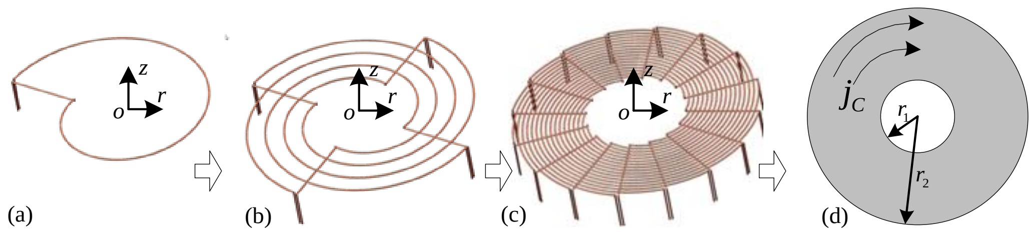

Figure 3. Drive-coil configuration and its equivalent model

Consequently, the plasma current sheet and the drive coil can be treated as two conductive disk shown in Figure 4

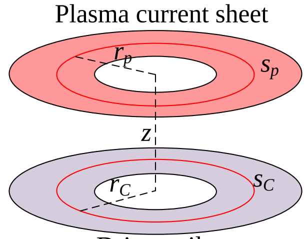

Figure 4. Equivalent model for *M* calculation

Taking two arbitrary filamentary current $\mathbf{S}_p$ and $\mathbf{S}_c$ on each disk, their mutual inductance can be calculated by Neumann's formula:

$$M_{pC} = -\mu_0 \sqrt{r_p r_C}[(\lambda - \frac{2}{\lambda})K + \frac{2}{\lambda}E] \tag{3}$$

$$\lambda = \frac{2\sqrt{r_p r_C}}{\sqrt{(r_p + r_C)^2 + z^2}} \tag{4}$$

$$K = \int_0^{\frac{\pi}{2}} \frac{\mathrm{d}\theta}{\sqrt{1 - \lambda^2 \sin^2\theta}} \tag{5}$$

$$E = \int_0^{\frac{\pi}{2}} \sqrt{1 - \lambda^2 \sin^2\theta}\, \mathrm{d}\theta \tag{6}$$

Then the magnetic flux that generated by $\mathbf{S}_C$ and linked to $\mathbf{S}_p$ is:

$$\varphi_{Cp} = M_{Cp} |S_C| \tag{7}$$

Subsequently, the total magnetic flux generated by drive-coil and linked to $\mathbf{S}_p$ is:

$$\phi_{Coil,p} = \int_{r_1}^{r_2} \varphi_{Cp}\, \mathrm{d}r_C \tag{8}$$

After that, the total magnetic flux generated by drive-coil and linked to plasma is:

$$\psi_{Coil,Plasma} = \frac{\int_{r_1}^{r_2} \phi_{Coil,p} \, \mathrm{d} r_p}{r_2 - r_1} \tag{9}$$

Consequently, the mutual inductance M between drive-coil and plasma can be calculated by the determination of mutual inductance:

$$M(z) = \frac{\psi_{Coil,Plasma}}{I_C} \tag{10}$$

Considering the geometry of spiral line, the equation above is amended as below:

$$M(z) = \xi^2 M(z) \tag{11}$$

$$\xi = \int_{R_1}^{R_2} \frac{1}{(r_2 - r_1)} \cdot \frac{r}{\sqrt{k^2 + r^2}} dr \tag{12}$$

The self-inductance L_C of drive-coil can be then computed by:

$$L_C = M(z \to 0) \tag{13}$$

The decreasing of M when z increases can be properly fitted by:

$$M(z) = L_C \exp(-\frac{z}{2z_0}) \tag{14}$$

where z_0 is generally defined as the electromagnetic decoupling length of drive-coil.

According to Faraday's law, the azimuthal electric field E_θ along an arbitrary filamentary loop in the plasma region obeys:

$$\int_S E_\theta \, \mathrm{d} s = 2\pi r_p E_\theta = \frac{d\phi_{Coil,p}}{dt} = M_{Coil,p} \frac{dI_C}{dt} \tag{15}$$

At t=0 of each discharge pulse, when the plasma has not been produced and its back effect on the circuit can be neglected, the circuit behaves as an ideal LCR system, whose dI_C/dt can be calculated be:

$$\frac{dI_C}{dt} = \frac{V_0}{L_0 + L_C} \tag{16}$$

where L_0 is the parasitic inductance and V_0 is the charge voltage of capacitor.

C. Lumped elementary slug model

The lumped elementary slug model has been widely used to estimate the performance of IPPTs [7,9], where the plasma is treated as a slug accelerated by the circuit and the plasma-circuit system is treated as a two stage transformer shown in Figure 5(a).

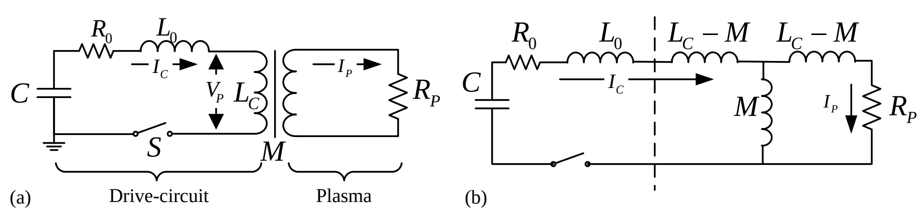

Figure 5. Transformer model of circuit-plasma system (a) and its equivalent circuit (b)

According to the equivalent circuit presented in Figure 5(b), the circuit equations can be derived as below:

$$\begin{cases} I_C R_0 + \frac{\mathrm{d}}{\mathrm{d}t}(L_0 I_c) + \frac{\mathrm{d}}{\mathrm{d}t}[(L_c - M)I_c] + \frac{\mathrm{d}}{\mathrm{d}t}[(I_c - I_p)M] - V_0 = 0 \\ \frac{\mathrm{d}}{\mathrm{d}t}[(L_c - M)I_p] + I_p R_p - \frac{\mathrm{d}}{\mathrm{d}t}[(I_c - I_p)M] = 0 \\ I_c = C\frac{\mathrm{d}V}{\mathrm{d}t} \end{cases} \tag{17}$$

The EM force of two coupling current sheet can be computed by:

$$F_l = I_c I_p \frac{\mathrm{d}M}{\mathrm{d}t} = \frac{1}{2}\frac{L_C}{z_0} I_c I_p \exp\left(\frac{z}{2z_0}\right) \tag{18}$$

Then, the motion equation of the plasma current sheet slug is:

$$m_{bit}\frac{\mathrm{d}u}{\mathrm{d}t} = \frac{1}{2}\frac{L_C}{z_0} I_c I_p \exp\left(\frac{z}{2z_0}\right) \tag{19}$$

(18) and (19) comprise the governing equations of the lumped elementary IPPT slug model, where the parameter L_C, z_0 and M(z) are calculated using (1)~(14).

III. Optimization result

Following the steps in Figure 2, the contour maps of E_θ and η under different r_1/r_2 values were calculated and shown in Figure 6. The results indicated that E_θ tended to be larger with smaller drive-coil dimension while η tended to be larger with larger drive-coil dimension. It was also interesting to find out that η maintained relatively high when the ratio of r_1/r_2 equaled 2/5. We have also computed the value of E_θ using identical theoretic method for PIT MK-I, which had demonstrated its performance to effective produce a magnetic-impermeable plasma current sheet using Argon. As a result, 12kV/m was adopted as the threshold of E_θ. Within the contour line of E_θ =12kV/m, the point (r_1=0.1m, r_2=0.25m) was found to have the highest η about 0.35 together with a proper I_{sp} about 2300s. The value of m_{bit} that can achieve this performance was about 0.75mg, which was adopted as the design goal of fast pulsed gas valve in another effort of our groupe[13,14].

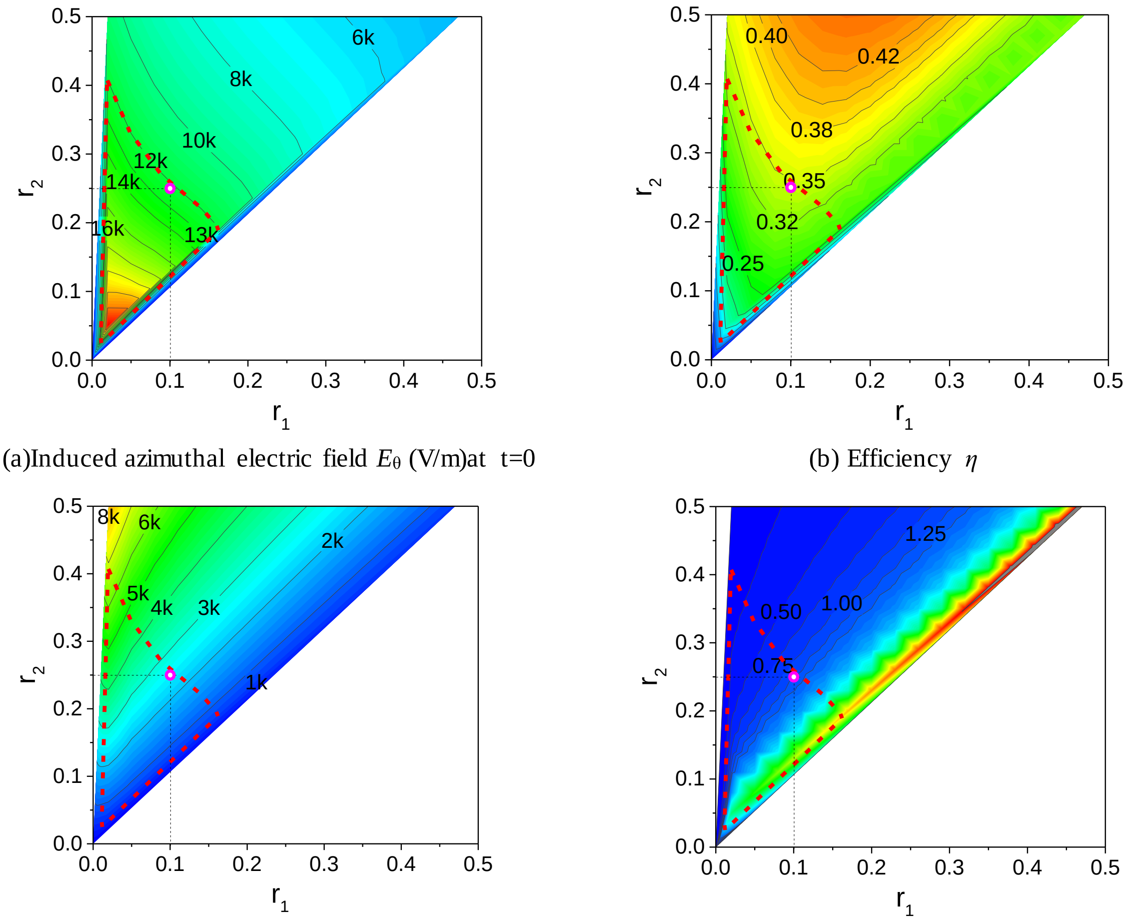

(a)Induced azimuthal electric field E_θ (V/m)at t=0

(b) Efficiency η

(c) Specific impulse I_{sp} (s)

(d) Propellant mass bit m_{bit} (mg)

Figure 6. Optimization result

IV. Numerical evaluation

The estimating of performance based on the lumped elementary slug model was relatively rough. To evaluate the design result, a two-dimensional magnetohydrodynamic model coupled with drive-circuit was employed to simulate the working process. This numerical model had demonstrated its validity and veracity to simulate an IPPT in our earlier research works[12,17]. The model, as is shown in Figure 7, treated the plasma, drive-coil and their surroundings as conjunctive computational domains. The magnetic field equation was solved in all the domains, while the Navier-Stokes equations and magnetic field equation are solved in a coupled way to capture the magnetohydrodynamic process of plasma only in the plasma domain. The current density distribution was computed based on the geometry of drive-coil and the current of circuit. The circuit current is solved by circuit equations. Plasma model is also solved to provide real-time plasma properties.

Simulation result provided a thrust impulse about 16.5mN s, the corresponding η was 31% and I_{sp} was 2240s. These performance parameters were slightly lower than that estimated by the lumped elementary slug model. This is because the slug model neglected many of the factors that may impair the acceleration of plasma, including the snowplow losses of plasma current sheet, the magnetic flux leakage through current sheet as well as the viscosity dissipation.

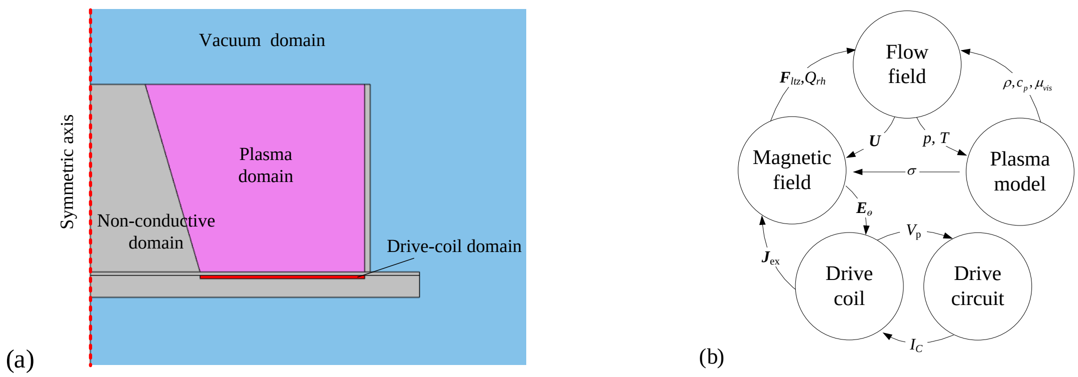

Figure 7. The circuit coupled MHD model: (a) model geometry; (b) parameter coupling relationship

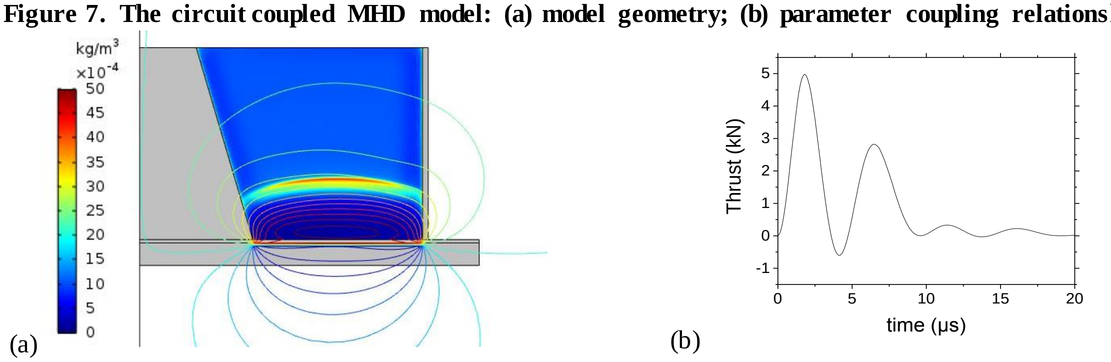

Figure 8. Simulation results: (a) ρ distribution and B_r contours at t=5μs; (b) total Lorentz force vs. time.

V. Conclusions

The drive-coil dimension of an inductive pulsed plasma thruster with single pulse energy about 500J (8μF capacitor charge to 12kV) was optimized depending on the classical lumped elementary slug model and comprehensive considerations of drive-coil EM field properties. Numerical simulation with circuit-coupled MHD model confirmed the performance of the design result. The thruster adopting this drive-coil design was shown in Figure 9, for further details of the preliminary test works of that device, one may refers to another paper we proposed to IEPC 2019—"Design and primary experiments on the prototype of a 500J inductive pulsed plasma thruster" by Dr. Xiaokang Li.

Acknowledgments

The research works are supported by the National Natural Science Foundation of China (Grant No. 51306203), the Chinese Manned Space Engineering Project 921 (Grant No. 0503), and the Natural Science Foundation of Hunan Province (Grant No. 2018GG3592).

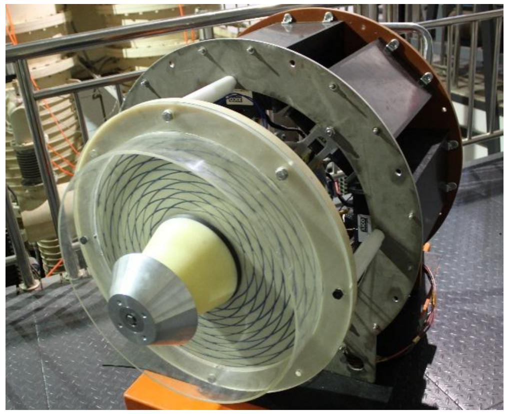

Figure 9. Photograph of the thruster accomplished

References

[1] *Polzin K A 2011 Comprehensive review of planar pulsed inductive plasma thruster research and technology J. Propul. Power 27 513–31(2011)*

[2] *Dailey C L 1965 Plasma properties in an inductive pulsed plasma accelerator 6th Biennial AIAA/Northwestern University Gas Dynamics Symposium (Evanston IL, August 1965) AIAA-1965-0637*

[3] *Dailey C L and Lovberg R H 1979 Large diameter inductive plasma thrusters 14th AIAA/DGLR International Electric Propulsion Conf.(Princeton NJ, 1979) AIAA-1979-2093*

[4] *Lovberg R H and Dailey C L 1982 A lightweight efficient argon electric thruster 16th AIAA/JSASS/DGLR International Electric Propulsion Conf.(New Orleans, LA, November 1982) AIAA-1982-1921*

[5] *Dailey C L and Lovberg R H 1993 The PIT MkV pulsed inductive thruster NASA Sti/recon Technical ReportN-93*

[6] *Russell D and Dailey C 2004 The PIT mark VI pulsed inductive thruster Space 2004 Conf. and Exhibit*

[7] *Martin A K 2016 Performance scaling of inductive pulsed plasma thrusters with coil angle and pulse rate J. Phys. D: Appl. Phys.*

[8] *R Lovberg and C Dailey. "Current Sheet Development in Pulsed Inductive Thruster" AIAA/ASME/SAE/ASEE 25th Joint Propulsion Conference AIAA89-2266 (1989)*

[9] *Martin A and Eskridge R 2005 Electrical coupling efficiency of inductive plasma accelerators J. Phys. D: Appl. Phys. 38 4168–79*

[10] *K A Polzin and Sankaran K 2013 Inductive pulsed plasma thruster model with time-evolution of energy and state properties J. Phys. D: Appl. Phys. 46 5201*

[11] *Mikellides P G and Neilly C 2007 Modeling and performance analysis of the pulsed inductive thruster J. Propul. Power 23 51–8*

[12] *Bi-xuan C, Mou-sen C, Xiao-kang L and Da-wei G "Physical mechanisms and factors influencing inductive pulsed plasma thruster performance: a numerical study using an extended magnetohydrodynamic model" J. Phys. D: Appl. Phys 51 365202 (2018)*

[13] *Dawei G, Mousen C and Xiaokang L "Design and test of a simple fast electromagnetic inductive gas valve for planar pulsed inductive plasma thruster" Review of Scientific Instruments. 2017, 88(10): 105101.*

[14] *Dawei G, Mousen C, Xiaokang L, et al. "Measurement of transient neutral gas puff pressure in NUDT_IPPTx by a fast ionization gauge" Plasma Science and Technology, 2018, 20(12): 125506.*

[15] *Dailey, C. L., and Lovberg, R. H.,"PIT Clamped Discharge Evolution," TRW Space and Technology Group, AFOSR-TR-89-0130, Redondo Beach, CA, Dec. 1988*

[16] *Mikellides P G and Neilly C 2007 Modeling and performance analysis of the pulsed inductive thruster J. Propul. Power 23 51–8*

[17] *Bi-xuan C, Mou-sen C, Xiao-kang L and Da-wei G "Physical mechanisms and factors influencing inductive pulsed plasma thruster performance: a numerical study using an extended magnetohydrodynamic model" J. Phys. D: Appl. Phys 51 365202 (2018)*